arXiv:cond-mat/0404185v1 [cond-mat.str-el] 7 Apr 2004

Large anomalous Hall effect in a silicon-based magnetic semiconductor

Ncholu Manyala[1,4], Yvan Sidis[1†], John F. DiTusa[1*], Gabriel Aeppli[2], David P. Young[1], and Zachary Fisk[3]

[1]Department of Physics and Astronomy,
Louisiana State University, Baton Rouge Louisiana 70803, USA
[2]London Centre for Nanotechnology and Department of Physics and Astronomy,
UCL, London WC1E 6BT, UK
[3]National High Magnetic Field Facility,
Florida State University, Tallahassee, Florida 32306, USA
[4]Department of Physics and Electronics,
National University of Lesotho, P.O. Roma 180, Maseru 100, Lesotho

[†]Present address Laboratoire Léon Brillouin,
CEA-CNRS, CE-Saclay, 91911 Gif-Sur-Yvette, France

Magnetic semiconductors are attracting high interest because of their potential use for spintronics, a new technology which merges electronics and manipulation of conduction electron spins. (GaMn)As and (GaMn)N have recently emerged as the most popular materials for this new technology. While Curie temperatures are rising towards room temperature, these materials can only be fabricated in thin film form, are heavily defective, and are not obviously compatible with Si. We show here that it is productive to consider transition metal monosilicides as potential alternatives. In particular, we

report the discovery that the bulk metallic magnets derived from doping the narrow gap insulator FeSi with Co share the very high anomalous Hall conductance of (GaMn)As, while displaying Curie temperatures as high as 53 K. Our work opens up a new arena for spintronics, involving a bulk material based only on transition metals and Si, and which we have proven to display a variety of large magnetic field effects on easily measured electrical properties.

Introduction

Magnetic semiconductors are attracting interest because they are more likely than ordinary metals to serve as injectors for spintronics applications. Recent successes include the discoveries that GaAs and GaN can display ferromagnetism on substitution of Ga by Mn[1–4]. GaAs and GaN are semiconductors with important uses in electro-optics, and the magnetism is clearly derived from the Mn ions while the carriers are derived from other dopants. Recent work has shown that the narrow gap[5,6] semiconductor FeSi can be doped via substitution of a single species, Co, for Fe to produce a low carrier density (n) magnetic metal with exceptional magnetoconductance (MC)[7]. That this is a truly itinerant low n system, in contrast to various semiconductors with Mn substitution, is apparent both from the absence of magnetism in the isostructural end members FeSi and CoSi of the $Fe_{1-y}Co_ySi$ dilution series, the fact that each Co atom adds one Bohr magneton to the magnetic polarization for low doping, and exceptional MC entirely understandable in terms of strong exchange enhancement of a disordered metal with Coulomb interactions[7,8]. In the present paper, we report the discovery of a large anomalous Hall effect (AHE) in addition to the other unusual properties already found for $Fe_{1-y}Co_ySi$. This is an important result because it demonstrates that large AHE may be a general feature of magnetic

semiconductors, and in particular can be found in low n, half-metallic materials with significant spin-orbit (SO) coupling evident in their band structures. Our measurements show that these diverse requirements can be achieved by simple chemical substitutions into a compound of two very common elements, iron and silicon.

1 Monosilicides

The monosilicides, FeSi, CoSi, and MnSi all have the same cubic B-20 crystal structure allowing the exploration of $Fe_{1-x}Mn_xSi$ and $Fe_{1-y}Co_ySi$ for all x and y between 0 and 1 (see Fig. 1)[9]. FeSi is fascinating in itself as a 'Kondo insulator', the designation for the insulating parents of the heavy fermion (HF) compounds. It transmits light in the far infra-red, with an optical gap of 60 meV, and originally attracted attention because, surprisingly, it has a response to external magnetic field which is large at room temperature but vanishes as the temperature approaches zero[5,6,10,11]. When doped with holes (Mn or Al) or electrons (Co) an insulator to metal (MI) transition occurs at a doping level of ~ 0.01 (see Fig. 1)[7,12,13]. While electron doping beyond the MI transition almost immediately produces a helimagnetic (HM) ground state, hole doping produces a simple paramagnetic (PM) metal[7,8,12].

MnSi has long been known[14] as a classic weak itinerant ferromagnet (FM), which continues to provide surprises in the area of metal physics[15,16]. Our $Fe_{1-x}Mn_xSi$ samples with $x \leq 0.8$ remain PM down to the lowest temperature (T) measured (1.7 K). In this article we focus on the HM phases and in particular on $Fe_{1-y}Co_ySi$ samples which are close in composition to the anomalous insulator FeSi. In this range of Co concentration, $y \leq 0.3$, magnetization measurements above 2 kG along with high field Hall effect measurements reveal that each Co dopant adds one Bohr magneton to the magnetic polarization[7] and one electron carrier to FeSi (Fig. 1d). We have concluded from these data that the electron gas

in these highly itinerant magnets is fully polarized at low temperature[7]. This means that by examining the transport and magnetic behavior across the $Fe_{1-x,y}Mn_xCo_ySi$ series, we can study the continuous evolution from a classic weak itinerant magnet, to a metallic paramagnet, to a Kondo (or strongly correlated) insulator, and finally a fully polarized itinerant magnetic metal[7,9,12] all without a change in crystal structure (see Fig. 1).

2 Experimental Results

Our main result of a large Hall resistivity (ρ_{xy}) in Co doped FeSi can be seen in Figs. 2 and 3. In Fig. 2 the magnetic field (H) dependence of ρ_{xy} of a few of our HM samples is displayed. As is common for ferromagnets and strong paramagnets, the Hall effect has two contributions, one proportional to H, which is the ordinary term from which we extract the carrier densities, and the second determined by $M(H)$ [17,18]. To highlight this second contribution it is customary to write ρ_{xy} as $\rho_{xy} = R_0H + 4\pi MR_S$. Here R_0 is the Hall effect resulting from the Lorentz force on the carriers in the same manner as in PM materials and R_S is referred to as the anomalous Hall constant. Thus in HMs and FMs at T below the Curie temperature (T_c), ρ_{xy} has roughly the same H dependence as the magnetization (M)[17,18]. This feature is demonstrated for $Fe_{1-y}Co_ySi$ in Figs. 2a and 3a where ρ_{xy} has a large linear field dependence below 2 kG, the field where M(H) saturates in Fig. 2c. Beyond 2 kG ρ_{xy} becomes much less field–dependent (Fig. 3a). At these high fields ρ_{xy} takes on the usual dependence on n and H, $d\rho_{xy}/dH = R_0 = 1/nec$ in its simplest form. It is for magnetic fields less than 2 kG that ρ_{xy} is proportional to M and the anomalous contribution dominates[17,18].

For comparison we have also plotted ρ_{xy} and M for our MnSi and $Fe_{0.1}Mn_{0.9}Si$ sample in Fig. 2. It is apparent from the figure that although M is of the same order and has a comparable H dependence, the Hall effect is vastly different for the Mn-rich and Co-

containing compounds. In fact there is a difference of a factor of 150 between the low H ρ_{xy} of the $Fe_{0.9}Co_{0.1}Si$ and $Fe_{0.1}Mn_{0.9}Si$ samples. We have chosen to compare these two samples in detail since they have the same crystal structure, the same level of chemical substitution, and HM ground states with $T_c = 10$ K.

A further comparison is shown in Fig. 2 b and d which presents the temperature dependence of the zero H resistivity (ρ_{xx}) and magnetic susceptibility (χ) at 50 G. Again, after the differences in Curie points have been taken into account, the magnetic properties of these samples appear to be similar. At the same time the temperature dependence of the resistivity is very different, ρ_{xx} rises above its trend line on cooling below T_c for Co-doped FeSi while it drops below the trend line as spin disorder scattering disappears for MnSi and Fe-doped MnSi. This effect has been discussed previously[7] in the context of greatly enhanced quantum interference effects in $Fe_{1-y}Co_ySi$. What interests us here is that our $Fe_{0.9}Co_{0.1}Si$ sample is 9 times more resistive than the $Fe_{0.1}Mn_{0.9}Si$ sample and nearly 20 times more resistive than MnSi. The differences in the two disordered alloys can be entirely accounted for in terms of the Drude model where the low T Hall mobility ($\mu_H = R_0/\rho_{xx}$) is essentially unchanged as a function of x and y (see Fig. 1e), and the carrier density is simply obtained from counting the surplus or deficit of valence electrons introduced by chemical substitution into the insulating FeSi parent compound. Perhaps this paradigm breaks down in the limit of pure MnSi, for which the mobility is larger by a factor of two, but, given the complexity of the band structure of the transition metal silicides[19], applies over a remarkably wide range of x and y, as does the tendency of R_0 to reflect the simple electron/hole counts associated with the chemical substitution (Fig. 1d). Given that the doped Kondo insulator $Fe_{1-y}Co_ySi$ behaves differently from the classic, high carrier density, itinerant manganese-rich compounds, we will compare our data to those for the classic ferromagnetic semiconductor, (GaMn)As, below.

To understand the origin of our results for ρ_{xy}, we now focus on the anomalous contribution to the Hall effect ($4\pi M R_S$), especially in the ordered state. The main part of Fig. 3a shows ρ_{xy} versus applied field on a scale strongly expanded relative to that of Fig. 2a. Since the saturation magnetization (M_S) of the $Fe_{0.1}Mn_{0.9}Si$ sample is ~ 3.5 times larger than M_S of our $Fe_{0.9}Co_{0.1}Si$ sample, R_S of these two compounds differ by a factor of ~ 500. The large Hall resistivity in $Fe_{1-y}Co_ySi$ is therefore predominantly controlled by the anomalous Hall coefficient. Fig. 3b shows how the anomalous term depends on temperature for some of our samples as well as (GaMn)As[2,3] with a T_c of 110 K. Although there is a difference of a factor of ~ 25 between R_S of $Fe_{1-y}Co_ySi$ and (GaMn)As, the temperature dependence of R_S in $Fe_{1-y}Co_ySi$ resembles that of (GaMn)As much more closely than those of the Mn-rich silicides. In particular, the data for $Fe_{1-y}Co_ySi$ and (GaMn)As have only slight temperature dependencies and converge on finite values as T goes to zero, while for the Mn-rich samples, R_S has a dramatic temperature dependence falling quickly toward zero as T goes to zero. We are thus left with a full Hall effect whose magnitude and temperature dependence is a much more sensitive probe of whether we are dealing with a magnetic semiconductor such as $Fe_{1-y}Co_ySi$ rather than an itinerant magnet like MnSi.

3 Discussion and Analysis

The commonly accepted theory of the AHE relies on SO coupling between the carrier and the lattice which produces a left-right asymmetry in the scattering[17,18]. Above T_c the randomization of the spins leads to an insignificant transverse electric field (E_y). However, a large E_y results when the material has a non-zero M due to the alignment of the carrier spins. The alignment creates an abundance of scattering in one particular direction, and a net current perpendicular to the longitudinal electric field. Thus an E_y many times

larger than that due to the Lorentz force is necessary to cancel this anomalous current. The usual description of R_S sums two contributions proportional to ρ_{xx} and ρ_{xx}^2 known as the "skew scattering" and "side-jump" terms respectively[17,18]. Since ρ_{xx} of our $x = 0.9$ and $y = 0.1$ samples differ by only a factor of ~ 9, this theory cannot account for the difference in R_S that we measure unless we posit that even though the scattering rates in these two materials are similar, the scattering in $Fe_{0.9}Co_{0.1}Si$ is much more effective in producing a perpendicular current.

What might account for the unusually large anomalous Hall effects for $Fe_{1-y}Co_ySi$, while leaving small values for isostructural MnSi? To explore this issue, it turns out to be useful to place our discoveries in a broader context. Fig. 4 compares the Hall effects for $H = 0.1$ T for $Fe_{1-y}Co_ySi$ and $Fe_{1-x}Mn_xSi$ to those for a wide range of other materials. As is well known and apparent in the figure, very large Hall effects result from making semiconductors intrinsic and thus reducing n. However, unlike the semiconductors, magnetic materials have large ρ_{xy} (as much as a few $\mu\Omega$ cm) while retaining both metallic n, and ρ_{xx}. In fact our $Fe_{1-y}Co_ySi$ samples have ρ_{xy} similar to nonmagnetic semiconductors with a factor of 250 times smaller n, while maintaining ρ_{xx} at a level 5 to 20 times smaller than these very clean crystalline semiconductors. (GaMn)As films in particular stand out as having very large Hall resistivities due in part to their small carrier concentrations ($n \sim 1.5 \times 10^{20}$ cm^{-3})[2]. What is also apparent is that our $Fe_{1-y}Co_ySi$ samples have among the largest ρ_{xy} measured at 4K for metallic (poly)crystalline FMs with moderate n.

Apart from going to low n, a second route to large Hall effects that enhances R_S is typically achieved in HF systems[20,21]. Fig. 4c, where we plot R_S against ρ_{xx}, makes clear that $Fe_{1-y}Co_ySi$ is comparable to other HF and mixed valent systems, with much higher n. However, what sets $Fe_{1-y}Co_ySi$ apart is that because it is a long-period HM rather than a PM, the field -induced magnetizations are much higher than for the PM

HF compounds.

What can be distilled from the first two frames of Fig. 4 is that $Fe_{1-y}Co_ySi$ follows the standard trend-lines of decreasing ρ_{xy} with n, but is shifted from the main line (of slope 1) describing ordinary semiconductors as well as (surprisingly) MnSi by a factor combining the high low field M of other FMs and an R_S as large as that of the HF systems.

Fig. 4c allows us to compare the anomalous Hall constant with other itinerant magnets as well. The upper half of this figure includes many of the half metallic materials, those with spin polarized Fermi gases, which have received a great deal of recent attention. This category includes the colossal magnetoresistive manganites[22], the half-Heusler materials[23], Sr_2FeMoO_6 [24] and $Fe_{1-y}Co_ySi$[7]. At the same time a large number of magnetic materials roughly follow the $R_S \propto \rho_{xx}^2$ law indicated by the red line in the figure.

For disordered materials, including the magnetic semiconductors of interest here, the second order term, or side-jump scattering, a virtual transition resulting in a transverse offset of the scattered wave functions, should dominate the AHE. However, as Jungwirth, Niu, and MacDonald point out[25] the theory of the side-jump term in R_S, originally introduced by Luttinger[26], does not depend on scattering to produce an effect. Instead, the AHE results from the change in the wave packet group velocity that occurs when electric fields are applied to a FM. As such it relies on the SO coupling inherent to the Bloch wave functions instead of the SO coupling to impurities or defects. Thus, it is a ground state property of the system and may account for the survival of the AHE down to low temperatures in materials such as (GaMn)As and $Fe_{1-y}Co_ySi$ (see Fig. 3)[2,3]. The relevant intrinsic quantity is the off–diagonal conductivity (σ_{xy}) and not the Hall resistance which also includes extrinsic scattering terms. We therefore plot (see Fig. 5) $\sigma_{xy} = \rho_{xy}/\rho_{xx}^2$ as a function of M for the same materials as in Fig. 4. Plotting the data in this way rather than the standard methods of Fig. 4, which are appropriate for extrinsic scattering dominated

off–diagonal conductivities, gives a new perspective on the different classes of materials. There are now three separate regions of behavior occupied by the HF materials (upper left corner), the carrier hopping systems (lower right corner), and the itinerant magnets which includes the magnetic semiconductors. One valuable insight which is gained immediately is that the colossal magnetoresistive manganites, in the carrier hopping region of the diagram, are truly distinct from the itinerant magnets.

The clear separation and general trends apparent in Fig. 5 suggest that such a plot can be highly valuable in characterizing the Hall effect mechanism and the importance of SO coupling to the carrier transport. Beyond occupying different regions of the diagram, there are very different trends for σ_{xy} versus M. In particular, the itinerant magnets show an obvious, monotonic increase in σ_{xy} with M, while the HF metals display a very dramatic rise in σ_{xy} with decreasing M; the general trend for the hopping systems is not so obvious[22,25,28]. For the HF metals, the behaviour is consistent with the $1/M^3$ law suggested, as spelled out in the figure caption, by a combination of two well known empirical facts about HFs, namely the Kadowaki-Woods relation and a constant Wilson ratio[27].

The itinerant magnets, including the magnetic semiconductors display a rough $\sigma_{xy} \sim M$ dependence which is especially clear for $Fe_{1-y}Co_ySi$ where all available data over a wide range of H and T are shown. Variations from this simple dependence evident in the data can be interpreted as a measure of the strength of the SO coupling from band structure effects[25]. Probably the most striking result is that the anomalous σ_{xy} in the HM monosilicides and the Mn doped III-V semiconductors shown in Fig. 5 are of comparable magnitude. Fig. 5 and Fig. 2c highlight the similarity of M of (GaMn)As and $Fe_{1-y}Co_ySi$ at low temperature despite the differences in the mechanisms producing the ferromagnetism. There are also large differences in n, 1.5×10^{20} cm^{-3} in (GaMn)As

and 4.4×10^{21} to 1.3×10^{22} cm^{-3} in $Fe_{1-y}Co_ySi$, and masses, $m^* = 0.5m_e$ and $0.08m_e$ for the heavy and light holes in (GaMn)As and $m^* = 30m_e$ in $Fe_{1-y}Co_ySi$[12,13]. However, the theory of Ref. (*25*) predicts that $\sigma_{xy} \propto m^*/n^{1/3}$, suggesting a trade-off between m^* and n that creates comparable σ_{xy} in these two FM semiconductors.

Fig. 5 also emphasizes that the differences between $Fe_{1-y}Co_ySi$ and MnSi are as profound as are the similarities of $Fe_{1-y}Co_ySi$ to (GaMn)As. Not only is the 5 K value an order of magnitude lower for MnSi, but σ_{xy} falls rather than rises as M approaches saturation on cooling.

4 Conclusions

To close, our work has five significant aspects. First, we have discovered a strongly correlated metal with a very large anomalous Hall effect. Second, we demonstrate that the large effect is most likely intrinsic - derived from band structure effects rather than due to impurity scattering. Third, the effect is not found for the isostructural MnSi, thus adding another[7] sharp distinction between classic weak itinerant ferromagnetism and semiconducting ferromagnets with nearly the same ordered moment and Curie temperature. Fourth, our survey of the Hall effect in a wide variety of materials of high current interest reveals that it can be more productive to look at the Hall conductivity than at the Hall resistance. Finally, our observation of the similarity of σ_{xy} in $Fe_{1-y}Co_ySi$ and (GaMn)As is another indication that doped Kondo insulators might be useful for spintronics and provides a strong point of contact between two major areas, namely magnetic semiconductors and strongly interacting Fermions. What makes FeSi especially attractive is that it is completely miscible with CoSi and MnSi and produces FMs with T_c's as large as 60 K[8], comparable to all but the highest T_cs of the variety of Mn doped III-V and II-VI semiconductors. There is now strong incentive to discover a doped Kondo insulator

exhibiting room temperature ferromagnetism.

5 Methods

Samples were either polycrystalline pellets or small single crystals grown from Sb and Sn fluxes. We produced the polycrystalline pellets by arc melting high-purity starting materials in an argon atmosphere. To improve the sample homogeneity the resulting $Fe_{1-y}Co_ySi$ ($Fe_{1-x}Mn_xSi$) samples were annealed for 24 hrs. at 1200 ^oC (four days at 1000 ^oC) in evacuated quartz ampoules. Powder x-ray spectra showed all samples to be single phase with a lattice constant linearly dependent on Co and Mn concentration (Fig. 1(c)). The linearity demonstrates that Co or Mn successfully replaces Fe over the entire concentration range ($0 \leq x \leq 1$, $0 \leq y \leq 1$). Energy dispersive x-ray microanalysis yielded results consistent with the nominal concentrations. The electrical conductivity and Hall effect were measured on rectangular samples with thin Pt wires attached with silver paste at 19 Hz using lock-in techniques. Finally, the magnetization measurements were made between 1.7 and 400 K in magnetic fields between -5.0 and 5.0 T in a SQUID magnetometer and from 0 to 32 T in a vibrating reed magnetometer at the NHMFL.

We thank D.A. Browne and J.Y. Chan for discussions. JFD, ZF, and GA acknowledge the support of NSF under contract No.s DMR 0103892, DMR 0203214, and a Wolfson-Royal Society Research Merit Award, respectively.

*To whom correspondence should be addressed; E-mail: ditusa@rouge.phys.lsu.edu.

1. Ohno, H., Munekata, H., Penney, T., von Molnar, S. & Chang, L.L. Magnetotransport properties of p-type (In,Mn)As diluted magnetic III-V semiconductors. *Phys. Rev. Lett.* **68**, 2664-2667 (1992).

2. Ohno, H. et al. (GaMn)As: A new diluted magnetic semiconductor based

on GaAs. *Appl. Phys. Lett.* **69**, 363-365 (1996).

3. Matsukura, F., Ohno, H., Shen, A. & Sugawara, Y. Transport properties and origin of ferromagnetism in (GaMn)As. *Phys. Rev. B* **57**, R2037-2040 (1998).

4. Reed, M.L. et al. Room temperature ferromagnetic properties of (GaMn)N. *Appl. Phys. Lett.* **79**, 3473-3475 (2001).

5. Schlesinger, Z. et al. Unconventional charge gap formation in FeSi. *Phys. Rev. Lett.* **71**, 1748-1751 (1993).

6. van der Marel, D., Damascelli, A., Schulte, K. & Menovsky, A.A. Spin, charge, and bonding in transition metal mono-silicides. *Physica B* **244**, 138-147(1998).

7. Manyala, N. et al. Magnetoresistance from quantum interference effects in ferromagnets. *Nature* **404**, 581-584 (2000).

8. Beille, J., Voiron, J. & Roth, M. Long period helimagnetism in the cubic-B20 $Fe_{1-x}Co_xSi$ and $Co_xMn_{1-x}Si$ alloys. *Sol. St. Comm.* **47**, 399-402 (1983).

9. Wernick, J.H., Wertheim, G.K. & Sherwood, R.C. Magnetic behavior of the monosilicides of 3d-transition elements. *Mat. Res. Bull.* **7**, 1431-1441 (1972).

10. Aeppli, G. & Fisk, Z. Kondo Insulators. *Comments Condens. Matter Phys.* **16**, 155-165 (1992).

11. Jaccarino, V., Wertheim, G.K., Wernick, J.H., Walker, L.R. & Arajs, S. Paramagnetic excited states of FeSi. *Phys. Rev.* **160**, 476-482 (1967).

12. DiTusa, J.F., Friemelt, K., Bucher, E., Aeppli, G. & Ramirez, A.P. Metal–insulator transitions in Kondo insulator FeSi and classic semiconductors are similar. *Phys. Rev. Lett.* **78**, 2831-2834 (1997) and **78**, 4309(E) (1997).

13. Chernikov, M.A. et al. Low temperature transport, optical, magnetic, and thermodynamic properties of $Fe_{1-x}Co_xSi$. *Phys. Rev. B* **56**, 1366-1375 (1997).

14. See e.g. Moriya, T. *Spin fluctuations in itinerant electron magnetism.*, edited by Fulde, P. (Springer–Verlag, Berlin, 1985).

15. Mena, F.P. et al. Heavy carriers and non-Drude optical conductivity in MnSi.*Phys. Rev. B* **67**, 241101 1-4 (2003).

16. Pfleiderer, C., Julian, S.R. & Lonzarich, G.G. Non-Fermi-liquid nature of the normal state of itinerant-electron ferromagnets. *Nature* **414**, 427-430 (2001).

17. See e.g., Campbell, I.A. & Fert, A. *Ferromagnetic Materials.*, Edited by Wohlfarth, E.P. (North-Holland Pub. Co., Amsterdam, 1982), Vol. **3**.

18. Maranzana, F.E. Contribution to the theory of the anomalous Hall effect in ferro- and antiferromagnetic materials. *Phys. Rev.* **160**, 421-429 (1967).

19. Mattheiss, L.F. & Hamann, D.R. Band Structure and Semiconducting Properties of FeSi. *Phys. Rev. B*, **47** 13114-13119 (1993).

20. Cattaneo, E. Hall–effect of Ce intermetallic compounds. *Z. Phys. B* **64**, 305-316 (1986).

21. Coleman, P., Anderson, P.W. & Ramakrishnan T.V. Theory of the anomalous Hall constant of mixed–valence systems. *Phys. Rev. Lett.* **55**, 414-417 (1985).

22. Matl, P. et al. Hall effect of the colossal magnetoresistance manganite $La_{1-x}Ca_xMnO_3$. *Phys. Rev. B* **57**, 10248-10251 (1998).

23. Otto M.J. et al. Half-metallic ferromagnets: II. Transport properties of NiMnSb and related inter-metallic compounds. *J. Phys. Condens. Matter* **1**, 2351-2360 (1989).

24. Tomioka, Y. et al. Magnetic and electronic properties of a single crystal of ordered double perovskite Sr_2FeMoO_6. *Phys. Rev. B* **61**, 422-427 (2000).

25. Jungwirth, T., Niu, Q. & MacDonald, A.H. Anomalous Hall effect in ferromagnetic semiconductors. *Phys. Rev. Lett.* **88**, 207208-1 - 4 (2002).

26. Luttinger, J.M. Theory of the Hall effect in ferromagnetic substances. *Phys. Rev.* **112**, 739-751 (1958).

27. Kadowaki, K. & Woods, S.B. Universal relationship of the resistivity and specific–heat in heavy-Fermion compounds. *Sol. St. Comm.* **58**, 507-509 (1986).

28. Ye, J. et al. Berry phase theory of the anomalous Hall effect: application to colossal magnetoresistance manganites. *Phys. Rev. Lett.* **83**, 3737-3740 (1999).

29. Emel'yanenko, O.V., Lagunova, T.S., Nasledov, D.N. & Talalakin, G.N. Formation and properties of an impurity band in n-type GaAs. *Fiz. Tver. Tela* **7**, 1315-1323 (1965).

30. Field, S.B & Rosenbaum, T.F. Critical behavior of the Hall conductivity at the Metal-Insulator Transition. *Phys. Rev. Lett.* **55**, 522-524 (1985).

31. Chapman, P.W., Tufte, O.N., Zook, J.D. & D. Long. Electrical properties of heavily doped silicon. *J. Appl. Phys.* **34** 3291-3294 (1963).

32. Leighton, C.,Terry, I. & Becla, P. Metallic conductivity near the metal insulator transition in $Cd_{1-x}Mn_xTe$. *Phys. Rev. B* **58**, 9773-9782 (1998).

33. Carter, G.C. & Pugh, E.M. Hall effect and transverse magnetoresistance in some ferromagnetic iron–chromium alloys. *Phys. Rev.* **152**, 498-504 (1966).

34. Dorleijn, J.W. Electrical conduction in ferromagnetic metals. *Philips Res. Repts.* **31**, 287-410 (1976).

35. Lavine, J.M. Extraordinary Hall-effect measurements on Ni, some Ni alloys,and ferrites. *Phys. Rev.* **123**, 1273-1277 (1961).

36. McGuire, T.R., Gambino, R.J. & Taylor, R.C. Hall effect in amorphous thin–film magnetic alloys. *J. Appl. Phys.* **48**, 2965-2970 (1977).

37. Canedy, C.L., Gong, G.Q., Wang, J.Q. & Xiao, G. Large magnetic hall effect in ferromagnetic Fe_xPt_{100-x} thin films. *J. Appl. Phys.* **79**, 6126-6128 (1996).

38. Lin, S.C.H. Hall effect in an amorphous ferromagnetic alloy. *J. Appl. Phys.* **40**, 2175-2176 (1969).

39. Bergmann, G. & Marquardt, P. Resistivity of amorphous ferromagnetic Fe_cAu_{1-c} alloys: Anisotropy and field dependence. *Phys. Rev. B* **18**, 326-337 (1978).

40. Pakhomov, A.B., Yan, X. & Zhao, B. Observation of giant Hall effect in granular magnetic films. *J. Appl. Phys.* **79**, 6140-6142 (1996).

41. Pakhomov, A.B., Yan, X. & Zhao, B. Giant Hall effect in percolating ferromagnetic granular metal–insulator films. *Appl. Phys. Lett.* **67**, 3497-3499 (1995).

42. Samoilov, A.V, Beach, G., Fu., C.C., Yeh, N.-C. & Vasquez R.P. Magnetic percolation and giant spontaneous Hall effect in $La_{1-x}Ca_xCoO_3$ ($0.2 \leq x \leq 0.5$). *Phys. Rev. B* **57**, R14032-14035 (1998).

43. Katsufuji, T., Hwang, H.Y. & Cheong, S-W. Anomalous Magnetotransport properties of $R_2Mo_2O_7$ near the magnetic phase boundary. *Phys. Rev. Lett.* **84**, 1998-2001 (2000).

44. Taguchi, Y. & Tokura, Y. Magnetotransport phenomena in a metallic ferromagnet of the verge of a Mott transition: $Sm_2Mo_2O_7$. *Phys. Rev. B* **60**, 10280-10283 (1999).

45. Batlogg, B. et al. Charge dynamics in $(LaSr)CuO_4$ - from underdoping to overdoping. *J. Low Temp. Phys.* **95**, 23-31 (1994).

46. Bucher, B. et al. Charge dynamics of Ce–based compounds: Connection between the mixed valent and Kondo–insulator states. *Phys. Rev. B* **53**, R2948-2951 (1996).

47. Lapierre, F. et al. Hall effect in heavy Fermion systems. *J. Mag. Mag. Mat.* **63 & 64**, 338-340 (1987).

48. Hadzic-Leroux, H. et al. Hall effect in heavy–Fermion systems: UPt_3, UAl_2, $CeAl_3$, $CeRu_2Si_2$. *Europhys. Lett.* **1**, 579-584 (1986).

49. Gao, Q.Z. et al. On the crystal field and Kondo effect in $CeIn_3$. *J. Mag. Mag. Mat.* **47 & 48**, 69-71 (1985).

50. Djerbi, R. et al. Influence of Y and La alloying on the anomalous Hall-effect of $Ce_2Ru_2Si_2$. *J. Mag. Mag. Mat.* **76 & 77**, 267-268(1988).

51. Kasuya, T. et al. in *Valence Fluctuations in Solids.*, Falicov, L.M., Henke, W. & Maple, M.B. (eds.) North-Holland Pub. Co. (Amsterdam), 281-284 (1981).

52. Penney, T. et al. Hall effect in the heavy Fermion systems $CeCu_6$ and UBe_{13}. *J. Mag. Mag. Mat.* **54 - 57**, 370-372 (1986).

Fig. 1. Phase diagram of $Fe_{1-x}Mn_xSi$ and $Fe_{1-y}Co_ySi$. (a)paramagnetic metallic (PMM), paramagnetic insulating (PMI) ($d\sigma/dT > 0$), and helimagnetic metallic (HMM) phases at zero field are displayed. (b) Conductivity (σ) at T = 2 K and H = 0 T vs. nominal Mn and Co concentration (x, y). (c) Lattice constant vs. x and y determined from powder X-ray diffraction measurements. (d) Carrier density as determined from Hall effect (for $H \geq 3$T) at 5.0 K vs. x and y. The line is a single carrier per Mn or Co atom behavior. (e) Hall mobility ($\mu_H = R_0/\rho_{xx}$) as determined from the line in (d) and zero field σ measurements at 5.0 K vs. x, y. The blue bullet is μ_H for MnSi where the high field Hall effect gives an apparent $n = 1.7 \times 10^{23}$ cm^{-3} large enough to exceed the scale in frame d.

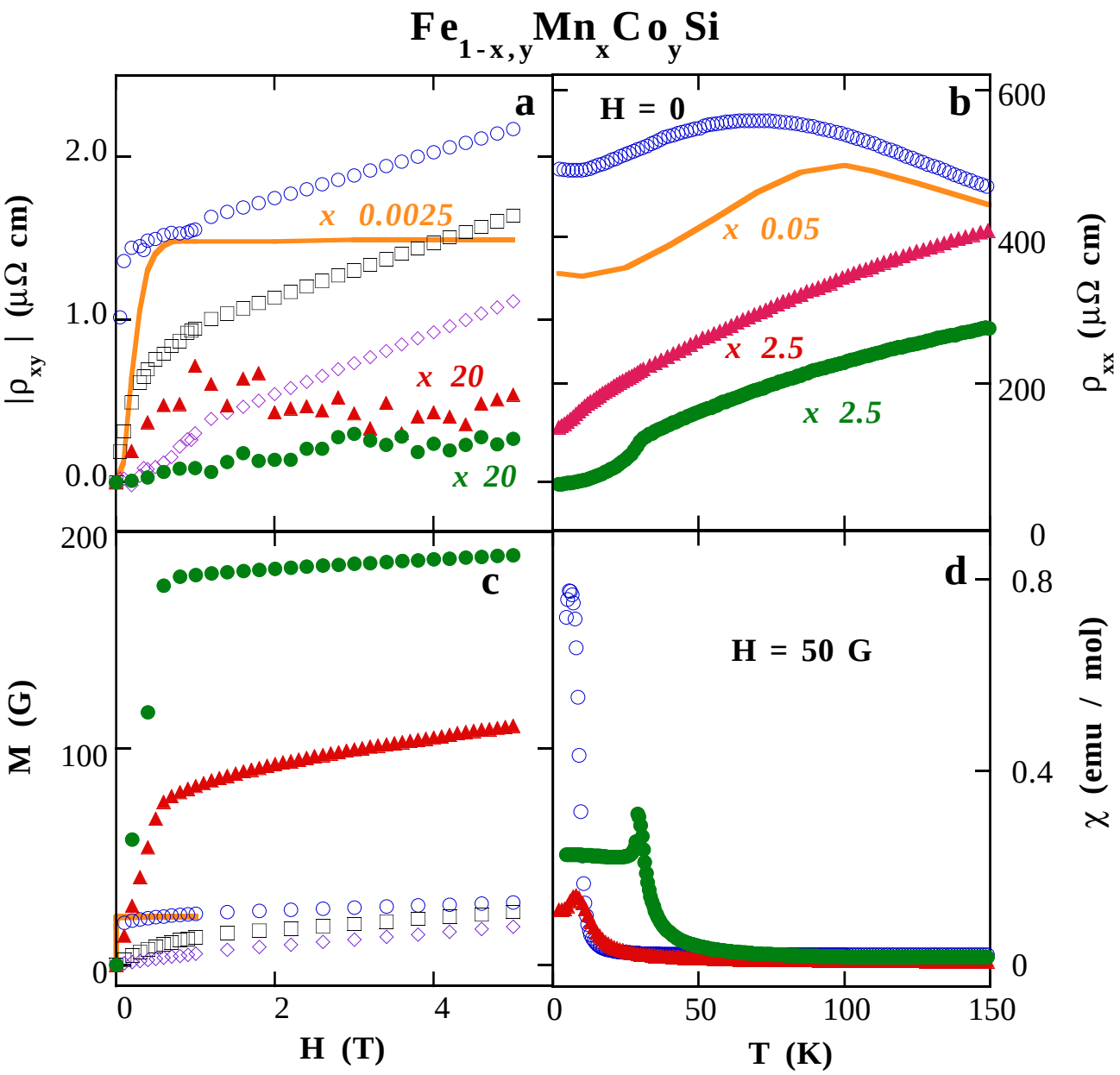
Fig. 2. Comparison of $Fe_{0.9}Co_{0.1}Si$, $Fe_{0.1}Mn_{0.9}Si$, MnSi, and $(Ga_{1-z}Mn_z)As$ ($z = 0.053$) taken from Refs. 2 & 3. (a) Hall resistivity (E_y/J_x) of $Fe_{0.9}Co_{0.1}Si$ at 5 K (blue circles), 15 K (black squares), and 25 K (purple diamonds), $Fe_{0.1}Mn_{0.9}Si$ at 5 K (red triangles), MnSi at 5 K (green bullets), and (GaMn)As at 2 K (orange line). (b) Resistivity at zero field of $Fe_{0.9}Co_{0.1}Si$ (blue circles), $Fe_{0.1}Mn_{0.9}Si$ (red triangles), MnSi (green bullets), and (GaMn)As (orange line). (c) Magnetization (symbols the same as in (a)). (d) Magnetic susceptibility at 50 G (symbols the same as (b)).

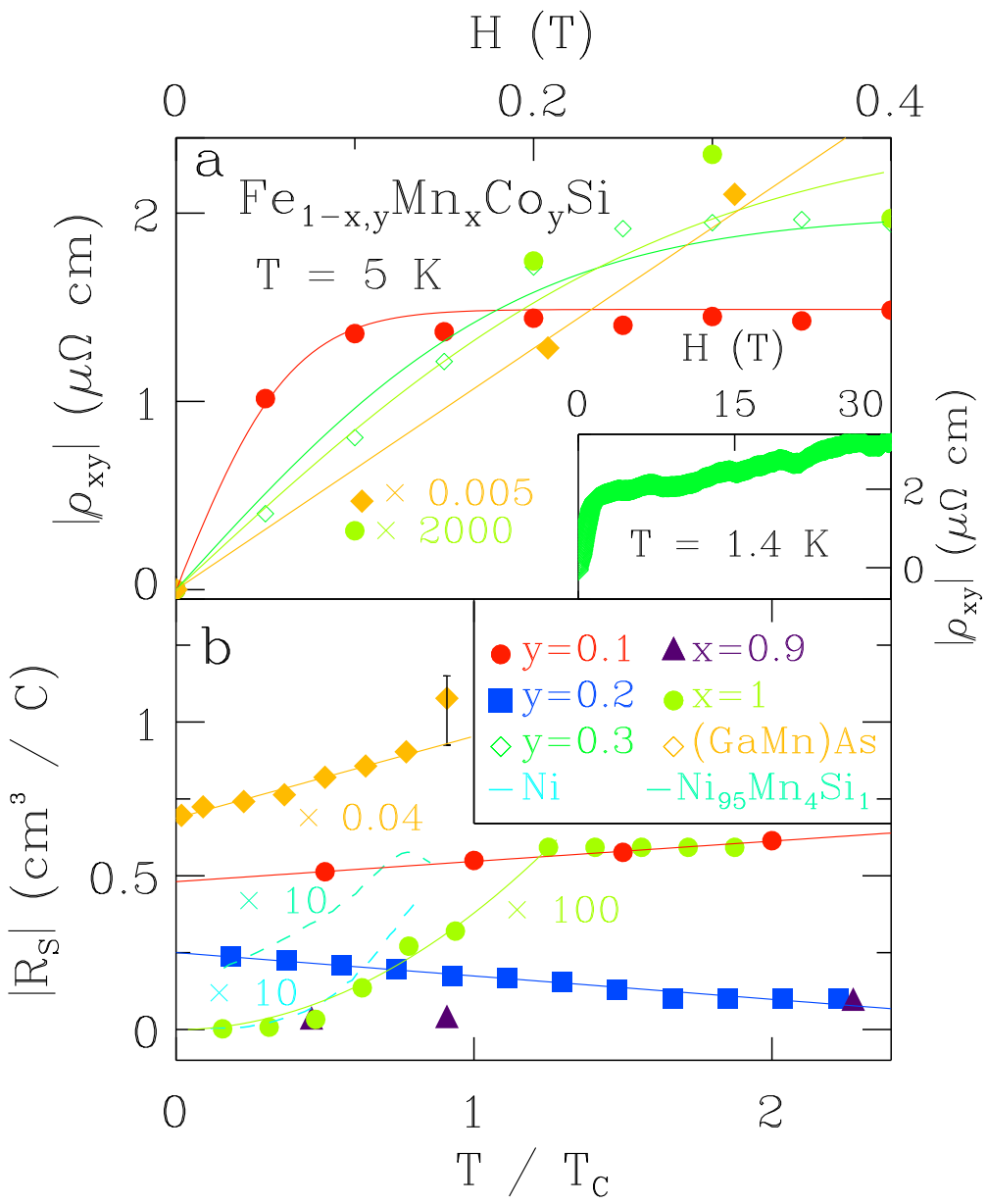
Fig. 3. Temperature and magnetic field dependence of the anomalous Hall effect. (a) Low field Hall resistivity (ρ_{xy}) vs. field for several $Fe_{1-y}Co_ySi$ and $Fe_{1-x}Mn_xSi$ samples. $y = 0.2$ sample is a single crystal. Symbols same as in (b). Inset: High field ρ_{xy} of our $y = 0.3$ sample. (b) Anomalous Hall constant (R_S) vs. temperature for several $Fe_{1-x}Mn_xSi$ and $Fe_{1-y}Co_ySi$ samples as well as $(Ga_{1-z}Mn_z)As$ ($z = 0.053$) taken from Refs. 2 & 3. Open symbols indicate T_c and lines are guides to the eye.

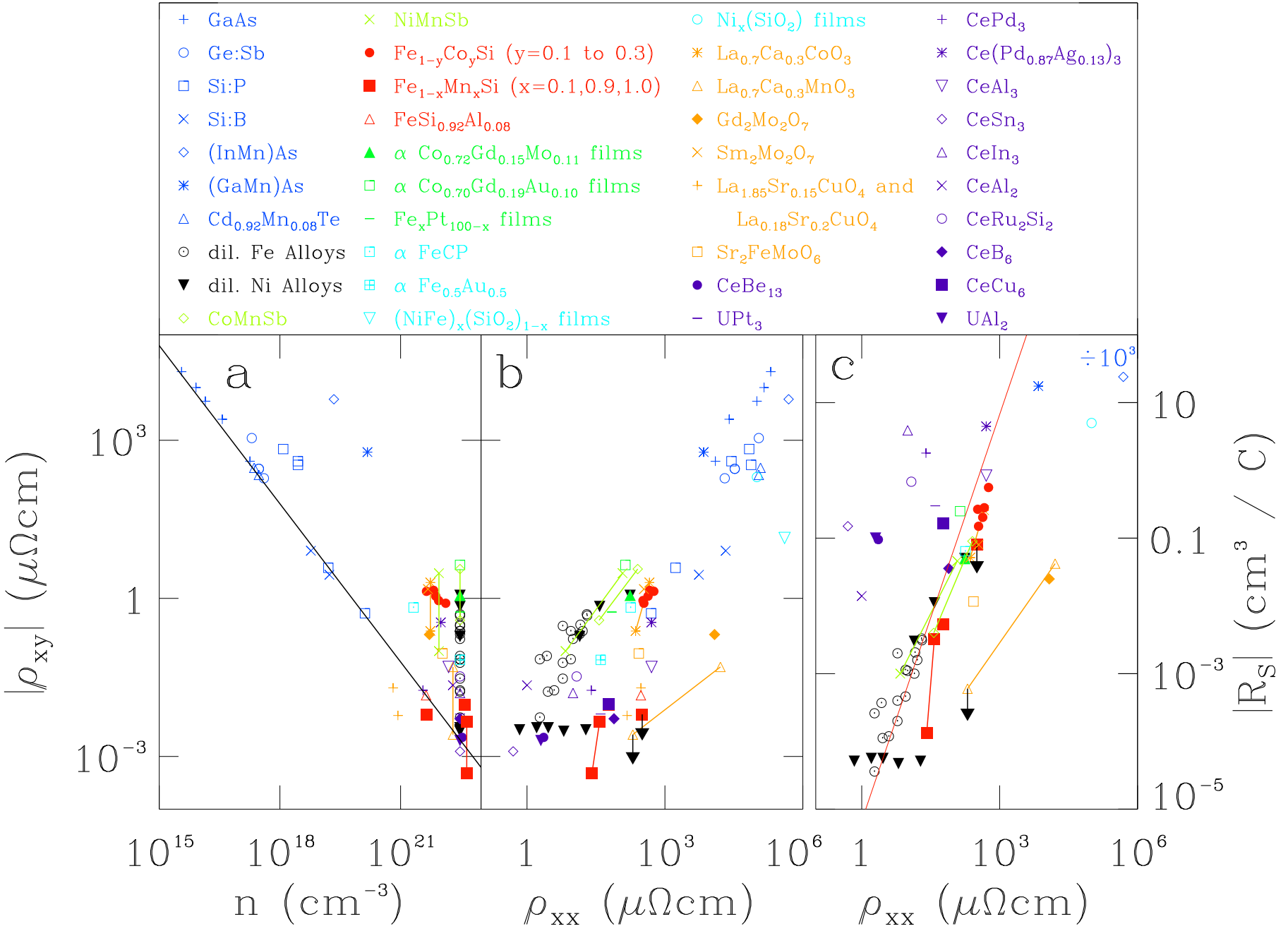
Fig. 4. Hall effect of paramagnetic metals and insulators, and ferromagnetic metals at 1 kG and low temperature. (a) Hall resistivity (ρ_{xy}) at 1 kG vs. carrier concentration (n) at ∼5 K except where noted below. Line is $\rho_{xy} = H/nec$, the Drude form. Data

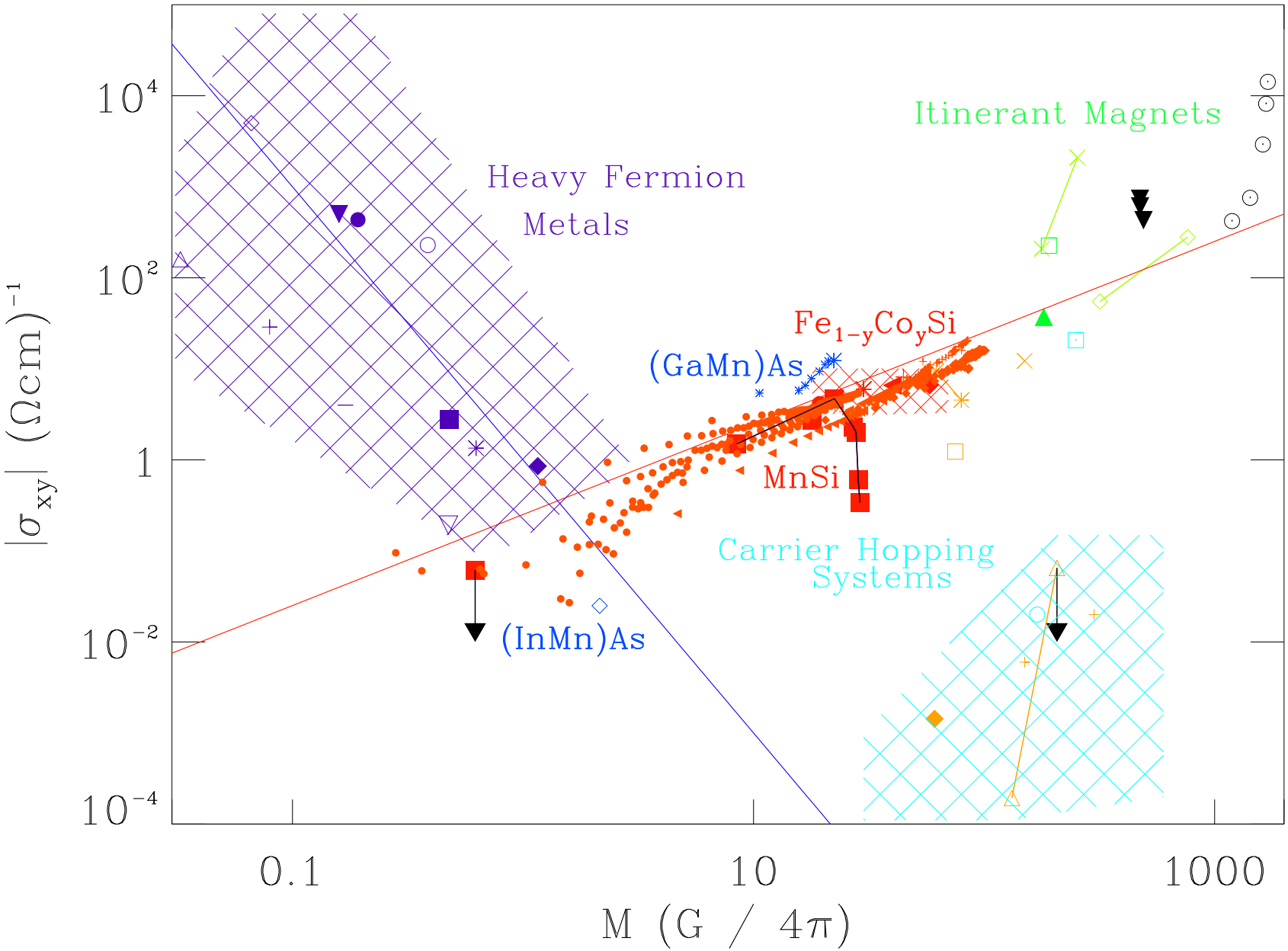
taken from the literature include GaAs[29], Ge:Sb[30], Si:P, Si:B[31], (InMn)As[1], (GaMn)As[2], $Cd_{0.92}Mn_{0.08}Te$[32], dilute Fe Alloys[33], dilute Ni Alloys[34,35], CoMnSb, NiMnSb[23], amorphous $Co_{0.72}Gd_{0.15}Mo_{0.11}$ films, amorphous $Co_{0.70}Gd_{0.19}Au_{0.10}$ films (77 K)[36], Fe_xPt_{100-x} thin film[37], amorphous FeCP[38], amorphous $Fe_{0.5}Au_{0.5}$[39], $(NiFe)_x(SiO_2)_{1-x}$ thin films[40], $Ni_x(SiO_2)$ thin films[41], $La_{0.7}Ca_{0.3}CoO_3$ (20 K)[42], $La_{0.7}Ca_{0.3}MnO_3$ (290 to 100 K)[22], $Gd_2Mo_2O_7$[43], $Sm_2Mo_2O_7$[44], $La_{2-x}Sr_xCuO_4$ ($x = 0.15, 0.2$)[45], Sr_2FeMoO_6[24], $CeBe_{13}$[20], UPt_3, $CePd_3$ and $Ce(Pd_{1-x}Ag_x)_3$[20,46], $CeAl_3$[47,48], $CeSn_3$[20], $CeIn_3$[49], $CeAl_2$[20], $CeRu_2Si_2$[50], CeB_6[51], $CeCu_6$[52], and UAl_2[47,48]. Lines connect data at different Ts for materials with strong T dependencies. (b) ρ_{xy} at 1 kG vs. resistivity (ρ_{xx}) at 5 K. (c) Anomalous Hall constant (R_S) vs. ρ_{xx} at 5 K. Line is a $R_S \propto \rho_{xx}^2$ behavior. Symbols with arrows denote an upper limit.

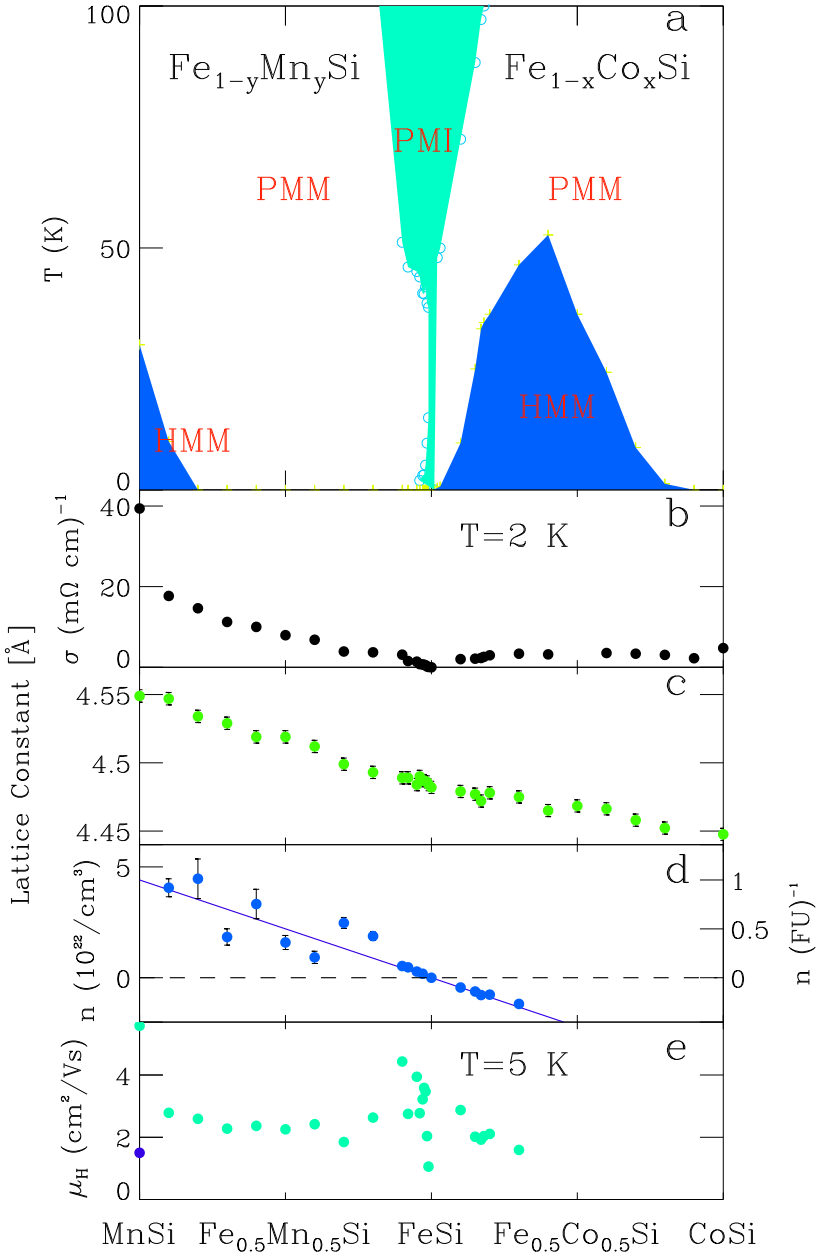
Fig. 5. Hall conductivity (σ_{xy}) of ferromagnetic metals and heavy Fermion materials. Symbols and references are as in Fig. 4, ie. collected at 1 kG and 5 K except where noted otherwise. Small dark–orange symbols are σ_{xy} for $Fe_{1-y}Co_ySi$ for $5 < T < 75$ K and $0.05 < H < 5$ T with $y = 0.01$ (bullets), $y = 0.15$ (solid–triangles), $y = 0.2$ (+), and $y = 0.3$ (solid–diamonds). Small blue asterisks are the (GaMn)As data for $5 < T < 120$ K from ref. *2*. Red line is $\sigma_{xy} \propto M$ demonstrating the leading M dependence of σ_{xy} for itinerant magnets. Purple line is a $1/M^3$ dependence predicted from a simple phenomenology of heavy Fermion materials. A decreasing σ_{xy} with M is most likely due to the stronger dependence of ρ_{xx} than M (for fixed H) on the effective mass in these compounds. We note that for HFs $\sigma_{xy} = \rho_{xy}/\rho_{xx}^2 \propto \chi_p H/A^2T^4$, where A is the coefficient of the Fermi liquid T^2 term in ρ_{xx} and χ_p is the enhanced Pauli susceptibility. The Kadowaki-Woods relation sets $A \propto \gamma^2 \propto \chi_p^2$ where γ is the coefficient of the linear T dependent term in the electronic specific heat and we have assumed a constant Wilson ratio (χ_p/γ)[27]. Thus we expect $\sigma_{xy} \propto \chi_p/\chi_p^4 \propto 1/M^3$ at low fields corresponding to the purple line.


Fe1-x,yMnxCoySi
a
b
c
d
H = 0
H = 50 G
x 0.0025
x 20
x 20
x 0.05
x 2.5
x 2.5
|ρxy| (μΩ cm)
ρxx (μΩ cm)
M (G)
χ (emu / mol)
H (T)
T (K)
2.0
1.0
0.0
600
400
200
0
200
100
0
0.8
0.4
0
0
2
4
0
50
100
150


H (T)
0
0.2
0.4
a
$Fe_{1-x,y}Mn_xCo_ySi$
T = 5 K
$|\rho_{xy}|$ ($\mu\Omega$ cm)
2
1
0
× 0.005
× 2000
H (T)
0
15
30
T = 1.4 K
2
0
$|\rho_{xy}|$ ($\mu\Omega$ cm)
b
y=0.1
x=0.9
y=0.2
x=1
y=0.3
(GaMn)As
Ni
$Ni_{95}Mn_4Si_1$
$|R_S|$ (cm³ / C)
1
0.5
0
× 0.04
× 10
× 100
× 10
0
1
2
T / T_C


GaAs
Ge:Sb
Si:P
Si:B
(InMn)As
(GaMn)As
$Cd_{0.92}Mn_{0.08}Te$
dil. Fe Alloys
dil. Ni Alloys
CoMnSb
NiMnSb
$Fe_{1-y}Co_ySi$ (y=0.1 to 0.3)
$Fe_{1-x}Mn_xSi$ (x=0.1,0.9,1.0)
$FeSi_{0.92}Al_{0.08}$
α $Co_{0.72}Gd_{0.15}Mo_{0.11}$ films
α $Co_{0.70}Gd_{0.19}Au_{0.10}$ films
Fe_xPt_{100-x} films
α FeCP
α $Fe_{0.5}Au_{0.5}$
$(NiFe)_x(SiO_2)_{1-x}$ films
$Ni_x(SiO_2)$ films
$La_{0.7}Ca_{0.3}CoO_3$
$La_{0.7}Ca_{0.3}MnO_3$
$Gd_2Mo_2O_7$
$Sm_2Mo_2O_7$
$La_{1.85}Sr_{0.15}CuO_4$ and
$La_{0.18}Sr_{0.2}CuO_4$
Sr_2FeMoO_6
$CeBe_{13}$
UPt_3
$CePd_3$
$Ce(Pd_{0.87}Ag_{0.13})_3$
$CeAl_3$
$CeSn_3$
$CeIn_3$
$CeAl_2$
$CeRu_2Si_2$
CeB_6
$CeCu_6$
UAl_2
a
b
c
÷10³
$|\rho_{xy}|$ (μΩcm)
$|R_S|$ (cm³ / C)
n (cm⁻³)
ρ_{xx} (μΩcm)
ρ_{xx} (μΩcm)


Heavy Fermion
Metals
Itinerant Magnets
Fe1-yCoySi
(GaMn)As
MnSi
Carrier Hopping
Systems
(InMn)As
10^4
10^2
1
10^-2
10^-4
|σxy| (Ωcm)^-1
0.1
10
1000
M (G / 4π)


a
$Fe_{1-y}Mn_ySi$
$Fe_{1-x}Co_xSi$
PMI
PMM
PMM
HMM
HMM
T (K)
100
50
0
b
T=2 K
σ (mΩ cm)$^{-1}$
40
20
0
c
Lattice Constant [Å]
4.55
4.5
4.45
d
n (10^{22}/cm^3)
5
0
n (FU)$^{-1}$
1
0.5
0
e
T=5 K
μ_H (cm^2/Vs)
4
2
0
MnSi
$Fe_{0.5}Mn_{0.5}Si$
FeSi
$Fe_{0.5}Co_{0.5}Si$
CoSi